Campos José Leandro Pereira Silveira (Orcid ID: 0000-0003-1578-8673)
Cruz Francisco William (Orcid ID: 0000-0002-4030-4581)
Ambrizzi Tercio (Orcid ID: 0000-0001-8796-7326)
Vuille Mathias (Orcid ID: 0000-0002-9736-4518)
Novello Valdir Felipe (Orcid ID: 0000-0002-0120-3745)
Strikis Nicolás Misailidis (Orcid ID: 0000-0003-4721-3380)

Coherent South American Monsoon Variability during the Last Millennium Revealed through high-resolution Proxy Records

J.L.P.S. Campos[1], F.W. Cruz[2], T. Ambrizzi[1], M. Deininger[3]; M. Vuille[4]; V.F. Novello[2]; N.M. Strikis[5]

[1] Department of Atmospheric Sciences, Instituto de Astronomia Geofísica e Ciências Atmosféricas, Universidade de São Paulo

[2] Department of Sedimentary Geology, Instituto de Geociências, Universidade de São Paulo

[3] Institute of Geosciences, Johannes Gutenberg University Mainz, J.-J.-Becher-Weg 21, 55128 Mainz, Germany

[4]Department of Atmospheric and Environmental Sciences, University at Albany, State University of New York

[5]Department of Geochemistry, Universidade Federal Fluminense

Corresponding author: José Campos (jose.leandro.campos@usp.br)

Key Points:

- We use high-resolution $\delta^{18}O$ records to decompose the South American monsoon into its main modes of variability during the last millennium.
- The first mode shows an enhanced monsoon during the Little Ice Age and a weakening during the Medieval Climate Anomaly.
- The second mode represents monsoon variability along the fringes of the monsoon area and indicates periods of widening/contractions of the monsoon axis.

This article has been accepted for publication and undergone full peer review but has not been through the copyediting, typesetting, pagination and proofreading process which may lead to differences between this version and the Version of Record. Please cite this article as doi: 10.1029/2019GL082513

Abstract

The number of paleo-precipitation records from the South American Monsoon domain that cover the last millennium has increased substantially in past years. However, hitherto most studies focused only on regional aspects, thereby neglecting the role of large-scale monsoon variability and the mechanisms that link proxy locations in space and time. Here we decompose the South American Monsoon into its main modes of variability by applying a Monte-Carlo Principal Component Analysis to a compilation of 11 well-dated summer paleo-precipitation records from tropical South America. The 1st mode represents changes in precipitation over the core monsoon domain, while the 2nd mode is characterized by high loadings along the fringes of the South American Monsoon over Southeastern South America and the northern monsoon limit. Composite analysis reveals an enhanced monsoon with a wider, rather than a southward-displaced, South Atlantic Convergence Zone during the early Little Ice Age, in contrast to previous interpretations.

Plain Language Summary

The South American Monsoon is responsible for more than 70% of the annual precipitation falling over tropical South America. Due to the lack of data prior to the middle of the 20th century, the long-term variability of the monsoon is poorly understood. Yet there are concerns that increasing greenhouse gas concentrations may significantly modify monsoon behavior in the 21st century. To better understand how the monsoon responds to such perturbations, detailed knowledge of how it varied in the past is crucial. This will facilitate improvements to Earth System Models that are used to project future rainfall changes in the region. Here 11 paleo-precipitation records that span the last millennium are analyzed using statistical techniques that allow extracting the shared variability from all records. Our result highlight how the monsoon responded in space and time to large-scale perturbations of the climate system, associated with the Little Ice Age and the Medieval Climate Anomaly.

1 Introduction

The tropical and subtropical South American climate is characterized by a monsoon circulation in austral summer, where the low-level winds converge over the eastern portion of the Amazon basin, transporting moisture westward into the continent. Blocked by the Andes, the flow forms a quasi-parallel "wind corridor" known as the northwest-southeast oriented South American Low-Level Jet (SALLJ), which, supported by midlatitudes transient weather systems, transports moisture from low to mid-latitudes (Zhou & Lau, 1998; Garreaud et al., 2009; Marengo et al., 2012; Vuille et al., 2012). Over the continental mid-latitudes (Paraguay and northern Argentina) a baroclinic thermal Low forms near the surface, the Chaco Low, leading to a cyclonic circulation over the La Plata Basin. This thermal Low, together with the anticyclonic circulation of the South Atlantic Subtropical High, supports the SALLJ and the low-level (850 hPa) moisture convergence, favoring deep convection, characterizing the monsoon axis or the South Atlantic Convergence Zone (SACZ, [*Kodama*, 1992]), schematically represented in Fig.1. The baroclinic upper level (300 hPa) counterparts to the Chaco Low and the subtropical High, the Bolivian High and an upper-level cyclonic vortex, known as the Northeast Trough [*Lenters et al*., 1999; *Chen & Schubert*, 1999], form an upper-level ridge (upper-level divergence region), which defines the position and shape of the monsoon axis.

The South American Monsoon is fueled by water vapor originating over the tropical Atlantic Ocean. The lack of a substantial temperature gradient during moisture transport across the tropical continent facilitates the application and interpretation of stable water isotopologues such as $\delta^{18}O$, suitable for paleo-precipitation studies within a Rayleigh distillation framework [*Vuille & Werner*, 2005; *Vuille et al*., 2012; *Hurley et al*., 2016; *Novello et al*., 2018]. During the last decade the number of available $\delta^{18}O$ records has increased significantly, resulting in a network of geographically well-dispersed records across the South American Monsoon area. Recent efforts to integrate multiple South American paleo-precipitation records have focused on the comparison of $\delta^{18}O$ time series across eastern Brazil, revealing a precipitation dipole across the SACZ region during last millennium [*Novello et al*., 2018; *Deininger et al*., 2019]. In general $\delta^{18}O$ records from speleothems, lake sediment calcite and ice cores in the tropical Andes [*Bird et al*., 2011; *Thompson et al*., 2012; *Kanner et al*., 2013; *Apaéstegui et al*., 2014] and south-central Brazil [*Novello et al*., 2016; *Novello et al*., 2018] contain a common signal that can be traced to their joint history of upstream rainout over the Amazon basin [*Vuille & Werner*, 2005; *Vuille et al*., 2012; *Hurley et al*., 2016]. At the same time multiple local calibration studies have also documented that these isotopic records are significantly correlated with local precipitation at the cave sites [e.g. *Moquet et al*., 2016; *Novello et al*., 2016]. Hence, we interpret changes in the $\delta^{18}O$ time series as variations in monsoon intensity, but also local hydrologic conditions at the respective locations where the proxies were sampled. These records all suggest that an anomalously drier climate prevailed during the Medieval Climate Anomaly (MCA, CE 950 – 1250, [*IPCC*, 2013]) and anomalously wetter conditions dominated the region during the Little Ice Age (LIA, CE 1450 – 1850, [*IPCC*, 2013]). In Northeastern Brazil (NEB) on the other hand, speleothems [*Novello et al*., 2012; *Novello et al*., 2018] indicate no changes in precipitation amounts during the MCA and a drier LIA, but a wetter transitional period (TRANS, CE 1250 – 1450, [*IPCC*, 2013]). However, a better characterization of the spatial and temporal coherence of monsoon variability as recorded in these discrete records is clearly needed, as is a more thorough analysis of the forcing mechanisms that are consistent with the observed monsoon variability in space and time. Here we provide an analysis of the spatio-temporal variability of the South American Monsoon, based on a quantitative decomposition of the existing records into two main modes of variability that explain most of the total variance observed during the past 1000 years. The analysis is based on a compilation of 11 well-dated paleoclimatic records from the South American Monsoon domain, employing the Monte Carlo Principal Component Analysis method [*Anchukaitis & Tierney*, 2013; *Deininger et al*., 2017].

2 Materials and Methods

In Table 1 and Fig. 1 the locations of the eleven $\delta^{18}O$ isotopic time series are presented (the records' time series are presented in supplementary Fig.1). Almost all records cover the period from CE 600 to CE 1970 (supplementary Table 1). The only exceptions are record #1 (PAL03+PAL04) and #4 (ALH+CUR4), which span up to CE 1928 and CE 1964 respectively. In order to extend these records to 1970, the alternate least squares algorithm was applied during the Principal Component Analysis. Some time series were obtained by merging two or three records as indicated in Table 1. In order to 'merge' these records, each isotopic time series was annually synchronized using a cubic spline during the overlap period. Each record was then normalized to unitary variance (z-scores) and averaged into one time

series. Finally, the time series was reconstructed using the inversion of the normalization of the longer time series (using standard deviation and the mean of the longer time series).

In order to account for the dating uncertainty of each proxy record, a linear age-depth model was constructed for each record accounting for ±1σ in the dating uncertainty. Through a set of 1000 Monte-Carlo simulations, where a random age within the ±1σ age interval was chosen each time, 1000 age models for each isotopic record were produced. The corresponding proxy time series were obtained through interpolation between the ages using the linear age-depth model (in the supplementary material a figure of the age-depth model is provided). Finally, each proxy time series was synchronized and sampled to an annual resolution before undergoing a low-pass filtering at the band of 30^{-1} $years^{-1}$, in order to account for differences in the records' original temporal resolution (for details see supplementary material).

Eleven time series, one for each record, were randomly chosen from the ensemble produced by the Monte-Carlo simulations, and subjected to a Principal Component Analysis (PCA), resulting in 11 spatial patterns (loading coefficients) and 11 principal components or scores (time series representing the standing oscillation of the spatial patterns). This procedure was repeated 1000 times, the number of Monte-Carlo simulations (see *Deininger et al*., 2017 and *Anchukaitis & Tierney*, 2013). More details on the methods are supplied in the supplementary material.

3 Results

3.1 Leading Modes of Monsoon Variability

The 1st and 2nd Monte-Carlo Principal Components were retained in this study, representing 30±2% and 13±1% of the total $\delta^{18}O$ variability (see supplementary Fig. 2), respectively. To compare the isotope-derived main modes of monsoon variability with present-day low-frequency precipitation patterns (Fig. 2, see supplementary Table 1 and supplementary Fig. 3 for details), a PCA of 110 years (CE 1901–2010) low-pass-filtered (>30 years) Total Column Rain Water (PC_{TCRW}) CERA-20C reanalysis data [20th Century Coupled European Reanalysis, [*Laloyaux et al*., 2018] was evaluated. The 1st and 3rd PC_{TCRW} spatial patterns (Loadings or Empirical Orthogonal Functions), explaining 42% and 13% of data variability, were associated (see supplementary Fig.7), with the 1st and 2nd $PC_{\delta^{18}O}$, respectively.

The spatial patterns of the 1st $PC_{\delta^{18}O}$ and the 1st PC_{TCRW} show similar spatial characteristics for most of the records analyzed (Fig. 2a). The leading mode derived from the $\delta^{18}O$ time series represents a dipole between the core monsoon region (blue colored dots, positive correlation) and the North and Northeast region of Brazil (brown colored dots). The latter is represented by the speleothems DV2, PAR and SBE. This dipole is consistent with the see-saw between the north-eastern and south-eastern portions of the South American Monsoon region suggested by *Novello et al.* [2018] and also seen in present day precipitation data (e.g. *Sulca et al.,* 2016). *Novello et al.* [2012] also showed that precipitation over the eastern Amazon varies in phase with precipitation over Northeastern Brazil and out of phase with isotopic proxies from the central Andes (#2-HUA and #3-QLC). A linear correlation in space between the 1st $PC_{\delta^{18}O}$ and the low-frequency TCRW data during the Current Warm Period (CWP, CE 1902-1970) results in very similar patterns (supplementary Fig. 6).

The 2nd $PC_{\delta^{18}O}$ shows a configuration, where proxy records in the southern tropical Andes (#2-HUA and #3-QUELC), and eastern Brazil (#8-SBE, #9-DV2) are positively

correlated with the 2nd $PC_{\delta^{18}O}$, while records from the more equatorial tropical Andes (#1-PAL, #11-PUM), the central Amazon (#10-PAR) and southeastern Brazil (#6-CRT) vary out of phase (Fig 2b). The remaining records (notably in the south-central Amazon) have small loading coefficients, indicating that they are not closely correlated with this mode. The 3rd PC_{TCRW} presents a similar pattern as seen in the proxy data (Fig 2b).

3.2 Time Series Analyses

The temporal variability of the two leading monsoon modes described above (Fig. 2) is represented by their respective principal components or time expansion coefficients (Fig. 3a,b). Negative values of these principal components indicate periods of positive precipitation anomalies at locations where the correlation between the principal component and the $\delta^{18}O$ time series is positive (Fig 2). A change point detection (CPD) test, based on the sample mean [*Lavielle,* 2005], was performed over the 1st and 2nd $PC_{\delta^{18}O}$. Five change points were detected for 1st $PC_{\delta^{18}O}$ (Fig. 3a), dividing the time series into four distinct climate periods or regimes. These periods can be assigned to the MCA (CE 724 -1160), a transitional period (TRANS, CE 1160 - 1489), the LIA (CE 1489 -1878) and the CWP. The same test was applied to the 2nd $PC_{\delta^{18}O}$ (Fig. 3b) as well as to the marine records of continental runoff from the La Plata basin and the Cariaco basin ([*Haug et al.*, 2001], Fig. 3d), respectively.

The dates of onset and demise of the identified climatic periods in this study differ from dates reported in the IPCC [2013], but these are based on Northern Hemisphere last millennium temperature, which may explain this discrepancy. Previous studies in South America [*Apaestegui et al.,* 2014; *Novello et al.,* 2012] used subjective criteria based on wavelet analysis, to determine the onset and the demise dates for these climate periods and came to different conclusions as well, particularly for the LIA period. This highlights the spatiotemporal variability in the timing of these climatic periods across tropical South America (further details can be found in supplementary Table 3).

4 Discussion

Given the strong similarity between the proxy- and the TCRW-derived leading modes, PC1 is interpreted as the monsoon variability mode, representing the spatio-temporal variability of convective activity over the core monsoon domain. This is because strong convective activity over the core monsoon region provokes an intensification of the east-west dipole, in turn reducing precipitation amounts in Northeastern Brazil (*Cruz et al.,* 2009; *Sulca et al.,* 2016), while precipitation amounts increase in the other monsoon regions. Furthermore, *Novello et al*. (2012) demonstrated that under such conditions, meridional ITCZ shifts become less influential in determining precipitation amounts in Northeastern Brazil. The variability of the 1st $PC_{\delta^{18}O}$ during the last millennium (Fig. 3a) shows strong excursions towards negative values during the LIA, indicating enhanced precipitation over the western, south-central and southeastern portions of tropical South America, balanced by reduced precipitation in northeastern South America, consistent with results from previous studies (see references in Table. 1 and *Deininger et al.* [2019]). During the MCA, positive values indicate reduced precipitation, with even stronger positive values in the period preceding the onset of the MCA.

The 2nd PC shows a pattern that is reminiscent of monsoon contraction and expansion with anti-phased precipitation behavior along the northern and southern edges of the

monsoon belt, when compared to its core region. We therefore interpret this PC as representing periods of monsoon widening or contraction, but we also caution that this mode is defined by few records along the fringes of the monsoon belt and that additional records will be required to develop a more robust picture of this mode of variability. The 2nd $PC_{\delta^{18}O}$ undergoes five regime shifts (Fig. 3b). The MCA and the 2nd half of the LIA (LIA2) are characterized by positive values, indicating dry anomalies over the northern monsoon border and over southeastern South America (regions with positive loadings in Fig 2b), whereas the early part of the LIA (LIA1) was anomalously wet in these regions.

The comparison with a precipitation reconstruction for the La Plata Basin from GeoB13813-4 [*Perez et al.,* 2016] (Fig. 3c), shows the same excursion toward wet anomalies (higher freshwater diatom percentage) during the LIA period as seen in the 1st $PC_{\delta^{18}O}$, indicative of a stronger monsoon. The La Plata drainage basin is a region that can receive high precipitation amounts during both strong and weak monsoon regimes. High runoff of the La Plata River can be caused by positive precipitation anomalies over the northern and southern portions of the basin, that are influenced by convective activity over the southwestern Amazon basin or mid-latitude transients and extreme SALLJ events during weak monsoon episodes, respectively [*Salio et al.,* 2007]. For example, a 'wet' excursion appears over the La Plata basin during the MCA, (labeled as event E-4 in Fig. 3c), despite dry anomalies over the northern portion of the La Plata basin, likely indicating a higher frequency of transient extra-tropical weather systems (e.g. cyclones, cold fronts and mesoscale convective systems).

The monsoon mode represents the dominant signal in the $\delta^{18}O$ data, indicating that the LIA was the wettest period over South America during the last millennium (event E-1 in Fig. 3a). The LIA signal is present in all time series, albeit with varying timing of onset and demise. The 2nd $PC_{\delta^{18}O}$, in particular shows an early onset and demise of the LIA. In the GeoB13813-4 sediment record the onset is delayed, but the demise is synchronous with the 1st $PC_{\delta^{18}O}$. The Cariaco %Ti record [*Haug et al.,* 2001] (Fig. 3d) is highlighting the displacement of the ITCZ, and is intimately tied to the SASM intensification (1st $PC_{\delta^{18}O}$,), consistent with the ITCZ-SASM relationship discussed in *Vuille et al.* (2012), although in the Cariaco %Ti record the LIA period ends a bit earlier (Fig. 3d).

The composite analysis for the LIA (E-1, Fig. 3e), CE 1489-1878, reveals wet anomalies over the core monsoon domain, including the southern Amazon, the tropical Andes and the SACZ, whereas stronger dry anomalies (> +1σ, see Supplementary Table 4) prevail over northern and northeastern Brazil (represented by records #9-DV2 and #10-PAR). The La Plata River Basin record (Fig. 3c) indicates enhanced fresh water input, consistent with its role as a proxy integrating the hydrologic response over a large watershed covering parts of the southern monsoon domain. Overall our result suggests that during the LIA, the South American Monsoon was enhanced, consistent with previous studies [*Bird et al.,* 2011; *Vuille et al.,* 2012; *Kanner et al.,* 2013; *Apaéstegui et al.,* 2014; *Deininger et al.* 2019].

The wettest period of the 2nd monsoon mode (Fig. 3b) occurred during the LIA1 period (event E-2). This period overlaps with the wettest period in the 1st $PC_{\delta^{18}O}$ (event E1, CE 1489-1639), a time when anomalously wet conditions dominate throughout the main monsoon domain (see composite in Fig. 3f). The only regions where conditions remained near average at this time are found over the La Plata basin, while northern and northeastern Brazil experienced dry conditions. The high-elevation Andean records Pumacocha (#1-PUM) and Quelccaya (#3-QLC) along the southwestern edge of the monsoon domain indicate wetter conditions at this time than during E-1, suggesting an enhancement of moisture

transport from the western Amazon basin to the Andes [*Garreaud et al.*, 2003; *Hurley et al.*, 2015]. The records #7-TMO and #8-SBE, located to the south of the NEB region, also present slightly wetter conditions than during the event E-1, indicating a northeastward expansion of the monsoon axis.

The MCA period is a more pronounced dry event in the 2nd $PC_{\delta}{}^{18}{}_{O}$ (event E-3, Fig. 3b) than in the 1st $PC_{\delta}{}^{18}{}_{O}$, but expressed as a wet event in in the GeoB13813-4 record (event E4, Fig. 3c). During this period drier conditions persist at almost all other locations, except Paraiso Cave, located in eastern Amazonia (#10-PAR), and Cristal Cave, located in southeastern Brazil (#6-CRT1). During this period, positive %Ti anomalies are recorded at the Cariaco Basin (Fig. 3d), consistent with the notion of a northward-displaced Atlantic ITCZ, evidencing again the relationship between monsoon intensity and the latitudinal position of the ITCZ [*Vuille et al.*, 2012] (see also supplementary Fig. 8). The "wet" pulse observed at that time in the GeoB13813-4 data (event E4) and in Cristal Cave, suggests higher activity of extra-tropical transient systems along the southern monsoon margin during this period.

Some authors, such as *Novello et al.* (2018) and *Bernal et al.* (2016), analyzed $\delta^{18}O$ and Sr/Ca composite means during the MCA and LIA, but considered only the latitudinal position of the records, which led them to suggest that a southward displacement of the SACZ or the monsoon axis took place during the LIA. However, the analysis of all existing isotopic records indicating South American Monsoon variability suggests an intensified SACZ associated with an enhanced monsoon preserved its shape throughout much of this period (Fig. 3f), except during its onset (E2, Fig. 3b). The enhancement of the monsoon during the LIA is directly connected to the southward shift of the ITCZ, which leads to an enhanced moisture influx from the tropical Atlantic towards tropical South America [*Vuille et al*, 2012], thereby enhancing the moisture convergence and convection over the monsoon region.

The subtropical South Atlantic represents another important monsoon forcing, forming a SST dipole between the tropical and subtropical South Atlantic, coupled to the overlying sea level pressure of the Subtropical High [*Chaves & Nobre*, 2004; *Jorgetti et al.*, 2014; *Utida et al.*, 2019]. When in its positive phase, the colder SSTs to the south and warmer SSTs equatorward, enhances the anticyclonic circulation associated with the Subtropical High and hence the inland moisture influx, thereby favoring the formation of the SACZ. In its negative phase, on the other hand, the Subtropical High is suppressed, favoring the intrusion of transient extratropical systems, such as extratropical cyclones and frontal systems, which lead to the characteristic northwest-southeastward orientation of the monsoon circulation over SESA. Unfortunately, the lack of high-resolution marine records from the last millennium in the South Atlantic precludes a more thorough assessment of the role of the South Atlantic in forcing the South American Monsoon during the last millennium (see *Utida et al.* [2019]).

In the current climate, when the monsoon axis is active, positive precipitation anomalies dominate over the SACZ domain, while precipitation is reduced over NEB and SESA [*Silva & Berbery*, 2006]. This occurs as the enhanced convection over the SACZ is balanced by increased subsidence over the surrounding regions and by the action of mid-latitude Rossby wave-trains propagating northeastward from the tropical Pacific Ocean in an arch-like trajectory [*Carvalho et al.*, 2004; *Muza et al.*, 2009; *Ma et al.*, 2011]. Such a pattern is observed during the LIA in event E2, where the NEB records (#10-DV2 and #11-PAR) present signals that are opposite to the core monsoon records, while the La Plata record

shows no significant anomalies (Fig.3f). However during the latter period of the LIA (E1) and the MCA (E3), (Figs. 3f,g), this pattern is not apparent, suggesting possible changes or displacements in the monsoon circulation and Rossby waveguides [*Hoskins & Ambrizzi*, 1993] during these times.

Wavelet and Spectral analyses (see supplementary material) were performed on the 1st and 2nd $PC_{\delta^{18}O}$ revealing significant periodicities at 256, 128, 70 and 32 years. Previous studies, such as *Novello et al.* [2012], *Apaestegui et al.* [2014], *Bernal et al.* [2016] and *Perez et al.* [2016], have argued that the longer cycle periodicities (128 and 256 years) can be attributed to solar variability and multidecadal internal variability such as the AMO (Atlantic Multidecadal Oscillation). Recent studies by *Jones and Carvalho* [2018] show a possible influence of the AMO on South American hydroclimate over the last 100 years. The AMO, in its positive phase, shifts the ITCZ northward following the warming of the subtropical North Atlantic, thereby increasing the cross-equatorial flow over northwestern South America and subsidence over northern Amazonia. This subsidence results in an enhancement of the meridional flow and more humid conditions over subtropical South America. Multiple studies have documented a past role of the AMO in modulating the South American Monsoon on multi-decadal time scales [*Chiessi et al.,* 2009; *Parsons et al.,* 2014]. Hence the AMO may have affected the behavior of the monsoon, especially during the MCA and LIA1 period, when the GeoB13013-4 (Fig. 3c) sediment record indicates exceptionally wet excursions during event E4 and at the beginning of event E2.

5 Conclusions

The Monte-Carlo Principal Component Analysis of 11 well-dated paleo-precipitation proxies from across tropical South America reveals two main modes of monsoon variability. The first mode is characterized by a southwest-northeast oriented dipole, representing monsoon strength over the core monsoon region, extending from the tropical Andes to eastern Brazil, with anti-phased monsoon strength in northeastern Brazil. This mode is associated with an enhanced monsoon during the LIA and a weakened monsoon during the MCA period. The second mode presents action centers toward the edges of the monsoon domain and therefore serves to characterize changes in the extent of the monsoon. This mode indicates drier conditions over southeastern South America during the early part of the LIA and wetter conditions during the late phase of the LIA.

Composite analyses and comparisons between the MC-PCA and the marine sediment record GeoB13813-4 [*Perez et al.,* 2016], representing the integrated precipitation over the La Plata Basin drainage area, suggest a widening of the monsoon domain during the early LIA period (CE 1489 – CE 1639). This result yields an alternative explanation to the spatio-temporal precipitation variability seen in the various (individual) proxy records, when compared to earlier studies which suggested that the SACZ or the monsoon axis was displaced southward during all the LIA [*Novello et al.,* 2018; *Apaéstegui et al.,* 2018; *Bernal et al.,* 2017; *Deininger et al.,* 2019].

The South American monsoon domain by now features a rich archive of spatially well-distributed high-resolution paleo-precipitation records covering the last millennium. This data set can now be exploited to analyze the multi-decadal evolution of monsoon precipitation and associated circulation systems such as the SACZ and the ITCZ. However, further efforts to recover additional paleo-precipitation records in under-sampled regions such

as Amazonia, northeastern Brazil and the La Plata Basin are needed, to further refine our understanding of the history of the South American Monsoon during the last millennium. Characterization and interpretation of the 2nd PC mode in particular, will benefit from further sampling along the edges of the monsoon domain. Oceanic SST proxies along the coast of Brazil would be equally valuable in this regard. Decomposing the monsoon into its main modes of variability by means of Monte Carlo Principal Component Analysis will also facilitate the comparison between paleoclimatic proxies and earth system models [*Benestad et al.*, 2017], slated to come online as part of the PMIP4/CMIP6 last millennium ensemble [*Jungclaus et al.*, 2017].

Acknowledgments, Samples, and Data

We are grateful to ICMBio for permission to collect stalagmite samples. J.L.P.S.C. was supported by CNPq/Brazil with fellowship 140140207/2017-1. The research received financial support from FAPESP/Brazil (grant PIRE FAPESP 2017/50085-3 to F.W.C. and fellowships 2016/15807-5 to V.F.N.; and INCLINE/USP to T.A. and F.W.C, and NSF OISE-1743738 to M.V. and 1103403 to R.L.E and H.C. MD acknowledges funding by the German Research Foundation (DFG) grant DE 2398/3-1. The authors especially wish to thank Prof. Pedro Silva Dias for his valuable comments on this manuscript. The proxy time series used in this paper can be found in the references of Table 1.

References

Anchukaitis, K. J., & Tierney, J. E. (2013). Identifying coherent spatiotemporal modes in time-uncertain proxy paleoclimate records. Climate Dynamics, 41(5-6), 1291-1306, https://doi.org/10.1007/s00382-012-1483-0

Apaéstegui, J., Cruz, F. W., Sifeddine, A., Vuille, M., Villar, J. C. E., Guyot, J. L., et al. (2014). Hydroclimate variability of the northwestern Amazon Basin near the Andean foothills of Peru related to the South American Monsoon System during the last 1600 years. Climate of the Past, 10(6), 1967-1981, doi: 10.5194/cp-10-1967-2014

Benestad, R., Sillmann, J., Thorarinsdottir, T. L., Guttorp, P., Mesquita, M. D. S., Tye, M. R., et al. (2017). New vigour involving statisticians to overcome ensemble fatigue. Nature Climate Change, 7(10), 697, https://doi.org/10.1038/nclimate3393

Bernal, J. P., Cruz, F. W., Stríkis, N. M., Wang, X., Deininger, M., Catunda, M. C. A., et al. (2016). High-resolution Holocene South American monsoon history recorded by a speleothem from Botuverá Cave, Brazil. Earth and Planetary Science Letters, 450, 186-196, https://doi.org/10.1016/j.epsl.2016.06.008

Bird, B. W., Abbott, M. B., Vuille, M., Rodbell, D. T., Stansell, N. D., & Rosenmeier, M. F. (2011). A 2,300-year-long annually resolved record of the South American summer monsoon from the Peruvian Andes. Proceedings of the National Academy of Sciences, 108(21), 8583-8588, https://doi.org/10.1073/pnas.1003719108

Bombardi, R. J., Carvalho, L. M., Jones, C., & Reboita, M. S. (2014). Precipitation over eastern South America and the South Atlantic Sea surface temperature during neutral ENSO periods. Climate Dynamics, 42(5-6), 1553-1568, https://doi.org/10.1007/s00382-013-1832-7

Carvalho, L. M., Jones, C., & Liebmann, B. (2004). The South Atlantic convergence zone: Intensity, form, persistence, and relationships with intraseasonal to interannual activity and extreme rainfall. Journal of Climate, 17(1), 88-108, https://doi.org/10.1175/1520-0442(2004)017<0088:TSACZI>2.0.CO;2

Chaves, R. R., & Nobre, P. (2004). Interactions between sea surface temperature over the South Atlantic Ocean and the South Atlantic Convergence Zone. Geophysical Research Letters, 31(3), https://doi.org/10.1029/2003GL018647

Chen, T. C., Weng, S. P., & Schubert, S. (1999). Maintenance of austral summertime upper-tropospheric circulation over tropical South America: The Bolivian high–Nordeste low system. Journal of the Atmospheric Sciences, 56(13), 2081-2100, https://doi.org/10.1175/1520-0469(1999)056<2081:MOASUT>2.0.CO;2

Chiessi, C. M., Mulitza, S., Pätzold, J., Wefer, G., & Marengo, J. A. (2009). Possible impact of the Atlantic Multidecadal Oscillation on the South American summer monsoon. Geophysical Research Letters, 36(21), https://doi.org/10.1029/2009GL039914

Cruz Jr., F.W., Vuille, M., Burns, S.J., Wang, X., Cheng, H., Werner, M., et al. (2009). Orbitally driven east-west anti-phasing of South American precipitation. Nature Geoscience, 2(3), 210-214, doi:10.1038/NGEO444.

Deininger, M., McDermott, F., Mudelsee, M., Werner, M., Frank, N., & Mangini, A. (2017). Coherency of late Holocene European speleothem $\delta^{18}O$ records linked to North Atlantic Ocean circulation. Climate Dynamics, 49(1-2), 595-618, https://doi.org/10.1007/s00382-016-3360-8

Deininger, M., Ward, B. M., Novello, V. F., & Cruz, F. W. (2019). Late Quaternary variations in the South American monsoon system as inferred by speleothems — New perspectives using the SISAL database. Quaternary, 2(1), 6, https://doi.org/10.3390/quat2010006

Garreaud, R. D., Vuille, M., Compagnucci, R., & Marengo, J. (2009). Present-day South American climate. Palaeogeography, Palaeoclimatology, Palaeoecology, 281(3-4), 180-195, https://doi.org/10.1016/j.palaeo.2007.10.032

Garreaud, R., Vuille, M., & Clement, A. C. (2003). The climate of the Altiplano: observed current conditions and mechanisms of past changes. Palaeogeography, Palaeoclimatology, Palaeoecology, 194(1-3), 5-22, https://doi.org/10.1016/S0031-0182(03)00269-4

Haug, G. H., Hughen, K. A., Sigman, D. M., Peterson, L. C., & Röhl, U. (2001). Southward migration of the intertropical convergence zone through the Holocene. Science, 293(5533), 1304-1308, doi: 10.1126/science.1059725

Hoskins, B. J., & Ambrizzi, T. (1993). Rossby wave propagation on a realistic longitudinally varying flow. Journal of the Atmospheric Sciences, 50(12), 1661-1671, https://doi.org/10.1175/1520-0469(1993)050<1661:RWPOAR>2.0.CO;2

Hurley, J. V., Vuille, M., & Hardy, D. R. (2016). Forward modeling of $\delta^{18}O$ in Andean ice cores. Geophysical Research Letters, 43(15), 8178-8188, https://doi.org/10.1002/2016GL070150

Hurley, J. V., Vuille, M., Hardy, D. R., Burns, S. J., & Thompson, L. G. (2015). Cold air incursions, $\delta^{18}O$ variability, and monsoon dynamics associated with snow days at Quelccaya Ice Cap, Peru. Journal of Geophysical Research: Atmospheres, 120(15), 7467-7487, https://doi.org/10.1002/2015JD023323

Jones, C., & Carvalho, L. M. (2018). The influence of the Atlantic multidecadal oscillation on the eastern Andes low-level jet and precipitation in South America. npj Climate and Atmospheric Science, 1(1), 40, https://doi.org/10.1038/s41612-018-0050-8

Jorgetti, T., da Silva Dias, P. L., & de Freitas, E. D. (2014). The relationship between South Atlantic SST and SACZ intensity and positioning. Climate Dynamics, 42(11-12), 3077-3086, https://doi.org/10.1007/s00382-013-1998-z

Jungclaus, J., Bard, E., Baroni, M., Braconnot, P., Cao, J., Chini, L., et al. (2017). The PMIP4 contribution to CMIP6 – Part 3: The last millennium, scientific objective, and experimental design for the PMIP4 past1000 simulations. Geoscientific Model Development, 10, 4005-4033, https://doi.org/10.5194/gmd-10-4005-2017

Kanner, L. C., Burns, S. J., Cheng, H., Edwards, R. L., & Vuille, M. (2013). High-resolution variability of the South American summer monsoon over the last seven millennia: insights from a speleothem record from the central Peruvian Andes. Quaternary Science Reviews, 75, 1-10, https://doi.org/10.1016/j.quascirev.2013.05.008

Kodama, Y. (1992). Large-scale common features of subtropical precipitation zones (the Baiu frontal zone, the SPCZ, and the SACZ) Part I: Characteristics of subtropical frontal zones. Journal of the Meteorological Society of Japan. Ser. II, 70(4), 813-836, https://doi.org/10.2151/jmsj1965.70.4_813

Laloyaux, P., de Boisseson, E., Balmaseda, M., Bidlot, J. R., Broennimann, S., Buizza, R., et al. (2018). CERA-20C: A coupled reanalysis of the Twentieth Century. Journal of Advances in Modeling Earth Systems, https://doi.org/10.1029/2018MS001273

Lavielle, M. (2005). Using penalized contrasts for the change-point problem. Signal Processing, 85(8), 1501-1510, https://doi.org/10.1016/j.sigpro.2005.01.012

Lechleitner, F. A., Breitenbach, S. F., Rehfeld, K., Ridley, H. E., Asmerom, Y., Prufer, K. M., et al. (2017). Tropical rainfall over the last two millennia: evidence for a low-latitude hydrologic seesaw. Scientific Reports, 7, 45809, https://doi.org/10.1038/srep45809

Lenters, J. D., & Cook, K. H. (1999). Summertime precipitation variability over South America: Role of the large-scale circulation. Monthly Weather Review, 127(3), 409-431. https://doi.org/10.1175/1520-0493(1999)127<0409:SPVOSA>2.0.CO;2

Ma, H. Y., Ji, X., Neelin, J. D., & Mechoso, C. R. (2011). Mechanisms for precipitation variability of the eastern Brazil/SACZ convective margin. Journal of Climate, 24(13), 3445-3456, https://doi.org/10.1175/2011JCLI4070.1

Marengo, J. A., Liebmann, B., Grimm, A. M., Misra, V., Silva Dias, P. L., Cavalcanti, I. F. A., et al. (2012). Recent developments on the South American monsoon system. International Journal of Climatology, 32(1), 1-21, https://doi.org/10.1002/joc.2254

Moquet, J.S., Cruz, F.W., Novello, V.F., Strikis, N.M., Deininger, M., Karmann, et al. (2016). Calibration of speleothem $\delta^{18}O$ records against hydroclimate instrumental records in Central Brazil. Global and Planetary Change, 139, 151-164.

Muza, M. N., Carvalho, L. M., Jones, C., & Liebmann, B. (2009). Intraseasonal and interannual variability of extreme dry and wet events over southeastern South America and the subtropical Atlantic during austral summer. Journal of Climate, 22(7), 1682-1699, https://doi.org/10.1175/2008JCLI2257.1

North, G. R., Bell, T. L., Cahalan, R. F., & Moeng, F. J. (1982). Sampling errors in the estimation of empirical orthogonal functions. Monthly Weather Review, 110(7), 699-706, https://doi.org/10.1175/1520-0493(1982)110<0699:SEITEO>2.0.CO;2

Novello, V. F., Cruz, F. W., Moquet, J. S., Vuille, M., de Paula, M. S., Nunes, D., et al. (2018). Two millennia of South Atlantic Convergence Zone variability reconstructed from isotopic proxies. Geophysical Research Letters, https://doi.org/10.1029/2017GL076838

Novello, V. F., Vuille, M., Cruz, F. W., Stríkis, N. M., De Paula, M. S., Edwards, R. L., et al. (2016). Centennial-scale solar forcing of the South American Monsoon System recorded in stalagmites. Scientific Reports, 6, 24762, https://doi.org/10.1038/srep24762

Novello, V. F., Cruz, F. W., Karmann, I., Burns, S. J., Stríkis, N. M., Vuille, M., et al. (2012). Multidecadal climate variability in Brazil's Nordeste during the last 3000 years based on speleothem isotope records. Geophysical Research Letters, 39(23), https://doi.org/10.1029/2012GL053936

Parsons, L. A., Yin, J., Overpeck, J. T., Stouffer, R. J., & Malyshev, S. (2014). Influence of the Atlantic Meridional Overturning Circulation on the monsoon rainfall and carbon balance of the American tropics. Geophysical Research Letters, 41(1), 146-151, https://doi.org/10.1002/2013GL058454

Perez, L., García-Rodríguez, F., & Hanebuth, T. J. (2016). Variability in terrigenous sediment supply offshore of the Río de la Plata (Uruguay) recording the continental climatic history over the past 1200 years. Climate of the Past, 12(3), 623-634, https://doi.org/10.5194/cp-12-623-2016

Salio, P., Nicolini, M., & Zipser, E. J. (2007). Mesoscale convective systems over southeastern South America and their relationship with the South American low-level jet. Monthly Weather Review, 135(4), 1290-1309, https://doi.org/10.1175/MWR3305.1

Silva, V. B., & Berbery, E. H. (2006). Intense rainfall events affecting the La Plata Basin. Journal of Hydrometeorology, 7(4), 769-787, 769-787, https://doi.org/10.1175/JHM520.1

da Silva, A. E., & de Carvalho, L. M. V. (2007). Large-scale index for South America Monsoon (LISAM). Atmospheric Science Letters, 8(2), 51-57, https://doi.org/10.1002/asl.150

Sulca, J., Vuille, M., Silva, Y., & Takahashi, K. (2016). Teleconnections between the Peruvian central Andes and Northeast Brazil during extreme rainfall events in austral summer. Journal of Hydrometeorology, 17, 499-515.

Thompson, L. G., Mosley-Thompson, E., Davis, M. E., Zagorodnov, V. S., Howat, I. M., Mikhalenko, V. N., & Lin, P. N. (2013). Annually resolved ice core records of tropical climate variability over the past~ 1800 years. Science, 340(6135), 945-950, DOI: 10.1126/science.1234210

Utida, G., Cruz, F.W., Etourneau, J., Bouloubassi, I., Schefuss, E., Vuille, M., et al. (2019). Tropical South Atlantic influence on Northeastern Brazil precipitation and ITCZ displacement during the past 2,300 years. Scientific Reports, 9, 1698, https://doi.org/10.1038/s41598-018-38003-6

Vuille, M., Burns, S. J., Taylor, B. L., Cruz, F. W., Bird, B. W., Abbott, M. B., et al. (2012). A review of the South American monsoon history as recorded in stable isotopic proxies over the past two millennia. Climate of the Past, 8(4), 1309-1321, https://doi.org/10.5194/cp-8-1309-2012

Vuille, M., & Werner, M. (2005). Stable isotopes in precipitation recording South American summer monsoon and ENSO variability: observations and model results. Climate Dynamics, 25(4), 401-413, https://doi.org/10.1007/s00382-005-0049-9

Wang, X., Edwards, R. L., Auler, A. S., Cheng, H., Kong, X., Wang, Y., et al. (2017). Hydroclimate changes across the Amazon lowlands over the past 45,000 years. Nature, 541(7636), 204, https://doi.org/10.1038/nature20787

Wortham, B. E., Wong, C. I., Silva, L. C., McGee, D., Montañez, I. P., Rasbury, E. T., et al. (2017). Assessing response of local moisture conditions in central Brazil to variability in regional monsoon intensity using speleothem 87 Sr/86 Sr values. Earth and Planetary Science Letters, 463, 310-322, https://doi.org/10.1016/j.epsl.2017.01.034

Zhou, J. and K. Lau, 1998: Does a Monsoon Climate Exist over South America?. Journal of Climate, 11, 1020–1040, https://doi.org/10.1175/1520-0442(1998)011<1020:DAMCEO>2.0.CO;2

Table 1 – Proxy records analyzed. Time series of the individual proxy records are provided in the supplementary material. The location of the records is illustrated in Fig.1.

Records	ID	Isotope	Lat	Lon	Mean Sampling	Reference
PAL03+PAL04	**1**	$\delta^{18}O_{cal}$	5.92°S	77.35°W	5.0 years	Apaestegui et al.2014
HUA	**2**	$\delta^{18}O_{cal}$	11.27°S	75.79°W	5.0 years	Kanner et al.2013
QUELC	**3**	$\delta^{18}O_{ice}$	13.93°S	70.83°W	1.0 year	Thompson et al. 2013
ALH+CUR4	**4**	$\delta^{18}O_{cal}$	15.20°S	56.80°W	0.6 year	Novello et al. 2016
JAR1+JAR4	**5**	$\delta^{18}O_{cal}$	21.08°S	55.58°W	2.5 years	Novello et al. 2018
CRT	**6**	$\delta^{18}O_{cal}$	24.58°S	48.58°W	2.7 years	Vuille et al. 2012
TMO	**7**	$\delta^{18}O_{cal}$	16.00°S	47.00°W	3.6 years	Wortham et al. 2017
SBE3+SMT5	**8**	$\delta^{18}O_{cal}$	13.81°S	46.35°W	1.2 years	Novello et al. 2018
DV2+TR5+LD12	**9**	$\delta^{18}O_{cal}$	12.36°S	41.57°W	4.0 years	Novello et al. 2014
PAR01+PAR03	**10**	$\delta^{18}O_{cal}$	4°4'S	55.45°W	7 years	Wang et al. 2017
PUM	**11**	$\delta^{18}O_{cal}$	10.07°S	76.06°W	1 year	Bird et al. 2011

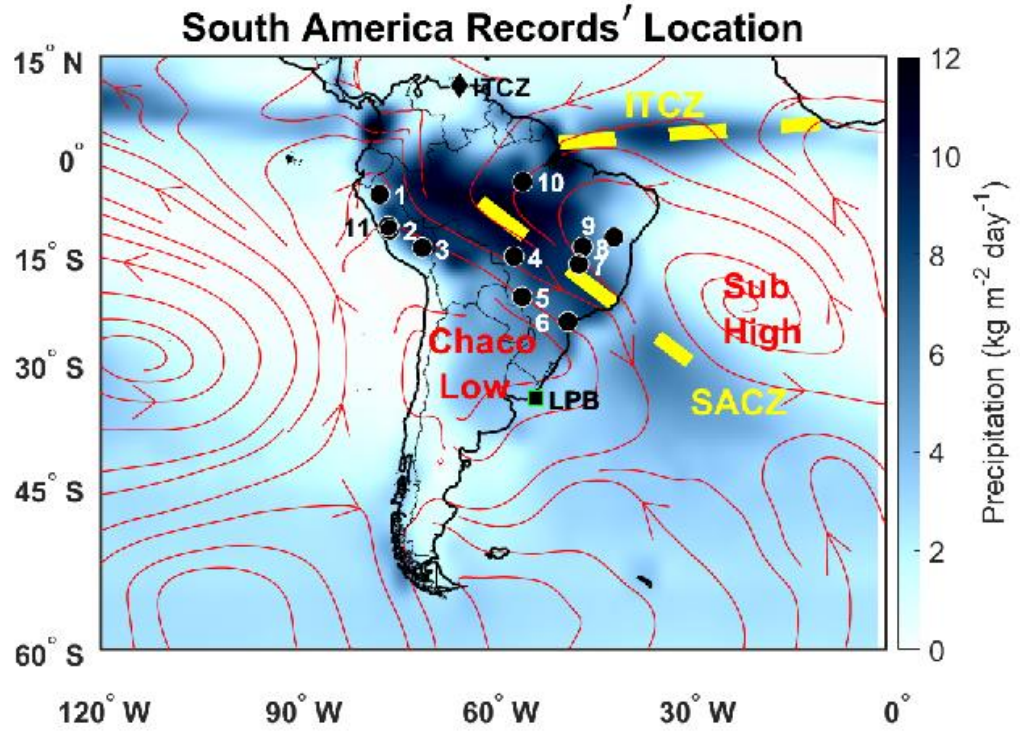

Figure 1 – 850 hPa monsoon circulation and location of isotopic proxy records used in the present study. The dots in the figure represent the record locations and the shading represents the mean summer (DJF) precipitation climatology extracted from 30 years (1981-2010 CE) of GPCP data. The red streamlines represent the austral summer (DJF) 850 hPa circulation. The ITCZ and SACZ are represented by the yellow dotted lines. The location of two non-isotopic marine records of continental runoff from the La Plata Basin (LPB) and the Cariaco Basin (ITCZ) are represented by a square and diamond, respectively.

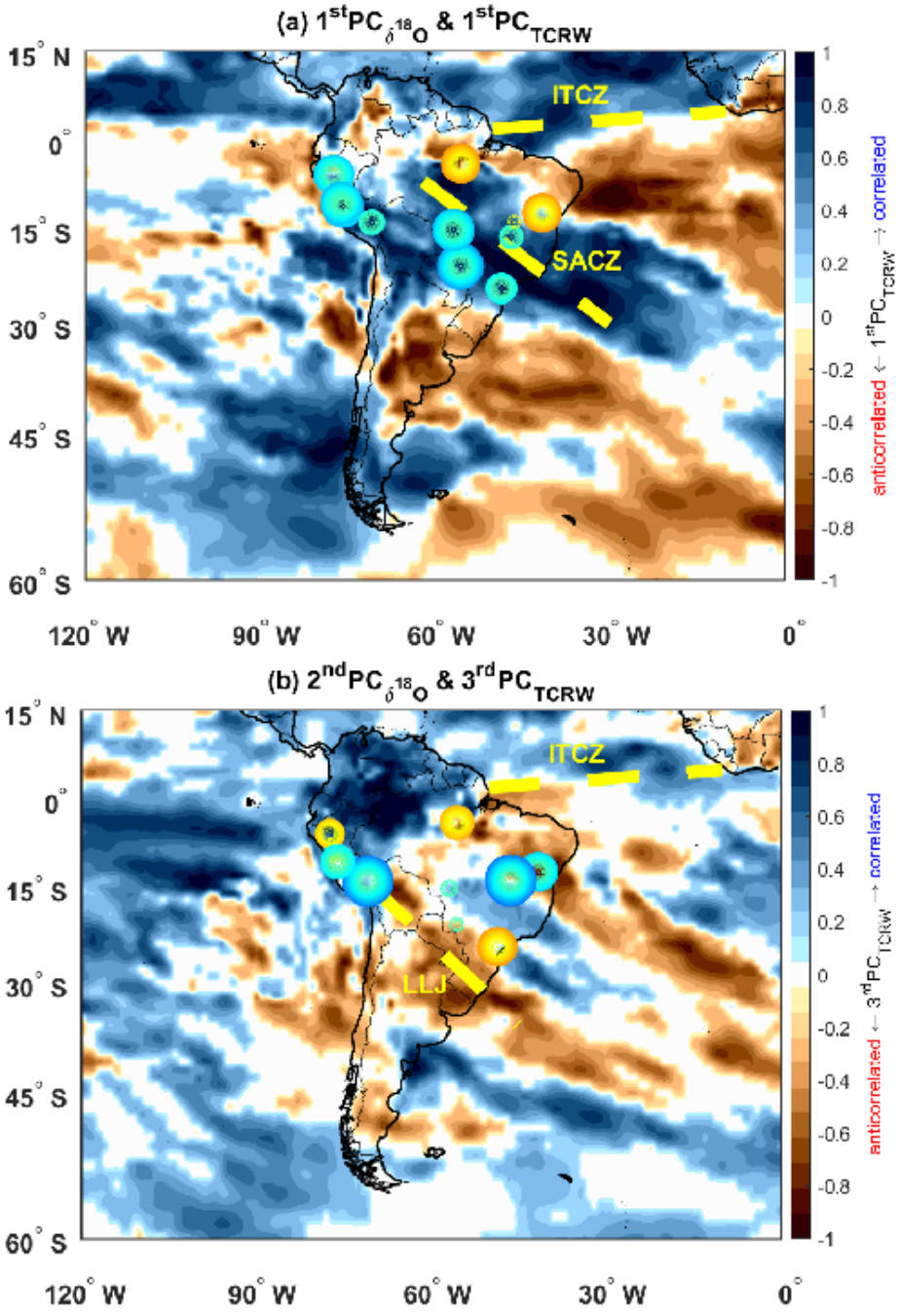

Figure 2–Comparison between proxy- and reanalysis-derived main monsoon modes. (a) 1st $PC_{\delta^{18}O}$ and (b) 2nd $PC_{\delta^{18}O}$. The dots in the figures represent the proxy records and the shading indicates the 1st and 3rd Principal Component computed with 110 years (CE 1901-2010) of CERA-20C Total Column Rain Water (TCRW) reanalysis data. The size of the dots corresponds to the loading coefficient magnitude, the blue and brown color represents positive and negative loadings of the $\delta^{18}O$ time series, respectively. The larger the dot, the stronger its correlation with the respective proxy-derived PC. The dashed yellow lines represent significant monsoon subcomponents, the ITCZ and the SACZ.

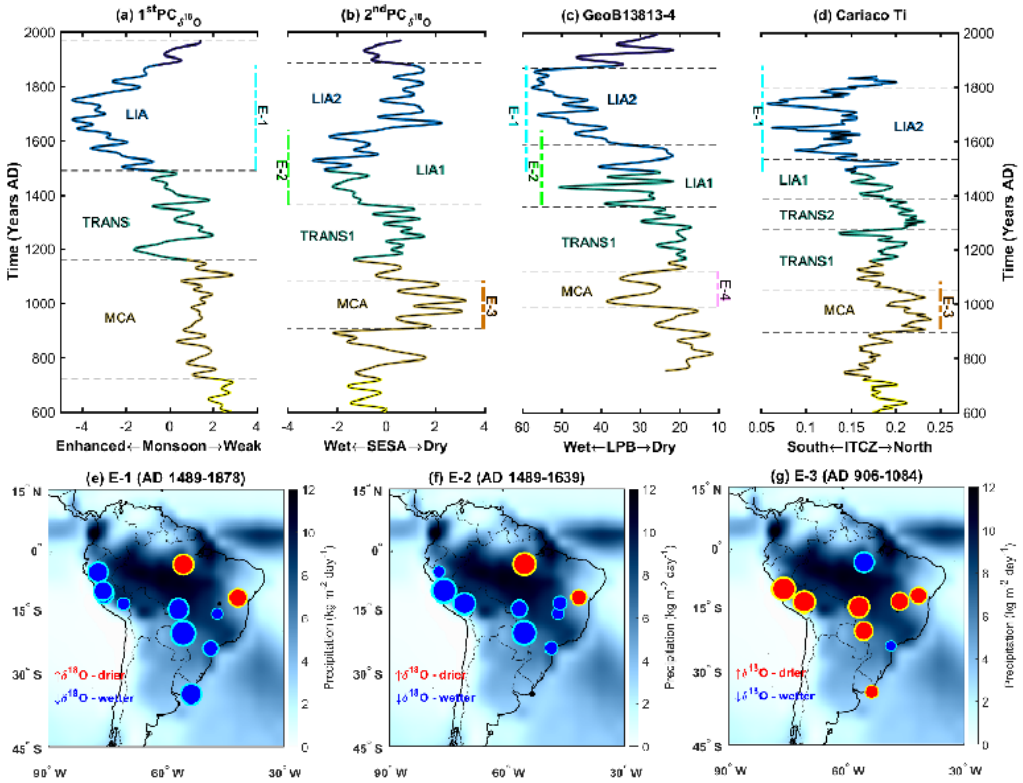

Figure 3 - Precipitation variability over South America during the Last Millennium. (a) 1st $PC_{\delta}{}^{18}{}_{O}$ mode, (b) 2nd $PC_{\delta}{}^{18}{}_{O}$ mode, (c) fresh water diatomaceous percentage on the La Plata river estuary [Perez et al. 2016] and (d) Cariaco Basin sediment Titanium ratio [Haug et al., 2001]. The colors represent the different climate regimes found through a change-point detection test based on the mean, evaluated on the 1st $PC_{\delta}{}^{18}{}_{O}$. The dotted lines represent change points detected with the respective time series. (e) Event 1 E-1, (f) Event 2 E-2 and (g) Event 3 E-3. The dots represent normalized $\delta^{18}O$ anomalies with respect to the period AD 600 – 1970, with red dots indicating positive $\delta^{18}O$ anomalies and blue dots negative $\delta^{18}O$ anomalies; the blue shading represents the mean precipitation climatology for the period CE 1980-2010. The marine sediment record GeoB13813-4 was also included in the maps.